Terrain Identification for RHex-type Robots

Camilo Ordonez[a] Jacob Shill[a] Aaron Johnson[b] Jonathan Clark [a] and Emmanuel Collins[a]

[a]Mechanical Engineering, Florida State University, Tallahassee, FL 31310, USA;
[b]Electrical and Systems Engineering, University of Pennsylvania, Philadelphia, PA 19104, USA

ABSTRACT

Terrain identification is a key enabling ability for generating terrain adaptive behaviors that assist both robot planning and motor control. This paper considers running legged robots from the RHex family, which the military plans to use in the field to assist troops in reconnaissance tasks. Important terrain adaptive behaviors include the selection of gaits, modulation of leg stiffness, and alteration of steering control laws that minimize slippage, maximize speed and/or reduce energy consumption. These terrain adaptive behaviors can be enabled by a terrain identification methodology that combines proprioceptive sensors already available in RHex-type robots. The proposed classification approach is based on the characteristic frequency signatures of data from leg observers, which combine current sensing with a dynamic model of the leg motion. The paper analyzes the classification accuracy obtained using both a single leg and groups of legs (through a voting scheme) on different terrains such as vinyl, asphalt, grass, and pebbles. Additionally, it presents a terrain classifier that works across various gait speeds and in fact almost as good as an overly specialized classifier.

Keywords: Legged robots, terrain identification

1. INTRODUCTION

Challenging robotic missions such as search and rescue, exploration, and surveillance to cite a few, usually take place on diverse and complex terrains. Therefore, it is imperative to develop methodologies that identify the terrain being (or to be) traversed by the robot and allow adjustments of motion plans, control strategies, and more specifically enable terrain dependent behaviors such as selection of gaits, modulation of leg stiffness, modification of robot morphology, and alteration of steering control laws that minimize slippage, maximize speed and/or reduce energy consumption.

Figure 1: XRL Experimental platform.

Terrain-based learning of the environment is now a relatively well developed field for wheeled ground vehicles, and is often divided into the subfields of terrain classification and terrain characterization (hereafter, we refer to these two groups as terrain identification). While terrain characterization generally refers to the determination of metrics such as roughness, slope and hardness,[1] terrain classification refers to approaches that give labels

Further author information: (Send correspondence to C.O.)
C.O.: E-mail: co04d@my.fsu.edu
J.S.: E-mail:jjs05e@my.fsu.edu
A.J.: E-mail:aaronjoh@seas.upenn.edu
J.C.: E-mail:jeclark@fsu.edu
E.C.: E-mail:ecollins@eng.fsu.edu

to the driving surfaces.[2] In addition, depending on the sensing methodology, the different techniques can be subdivided into either proprioceptive or vision-based approaches.[3]

However, terrain identification research is far less developed for legged systems that impose several challenges when compared to the wheeled counterparts. First, legged robots exhibit intermittent leg-terrain contact, which demand precise syncronization of the terrain identification algorithms with the step or stride of the robot. Second, legged robot dynamics change severely depending on the gait parameters.

Earlier work on terrain identification for slowly moving legged robots was motivated by the objective of guiding feet placement, and center of mass motion.[4,5] In both of these works, proprioceptive techniques were employed in conjunction with controlled experiments on single leg setups to classify and characterize terrains. A more recent work on vision based terrain classification includes the utilization of key, unique features in imagery data obtained from a camera mounted in the walking robot LittleDog.[6]

Previous work that is most closely related to our research, are the proprioceptive approaches employed by AQUA[7,8] and the six-legged dynamic running robot OctoRoACH.[9] The RHex[10] family robot AQUA, ultilized features derived from inertial data such as vertical acceleration, motor currents, and rate gyros at four prescribed leg angles during the stride of the robot. These features were used in conjunction with a probabilistic classifier and were evaluated on a littoral setting to detect the transition of the robot from the beach to the water in order to switch from a walking to a swimming gait . Additional experiments were conducted on snow, ice, and linoleum. It is important to note that during all experiments reported in,[7] the gait remained constant. More recent work on AQUA has studied the variations of the mentioned terrain features as a function of gait frequency. Preliminary results showed that there are particular leg frequencies that are optimal of terrain classification.[8] In the case of OctoRoACH, a Support Vector Machine (SVM) classifier was trained with features consisting of statistics (variance, skew, and kurtosis) obtained from time series from accelerometers, gyroscope, and motor back-EMF. The classifier was tested on carpet, gravel, and tile terrains. A clear dependency of the feature vectors on the stride frequency was observed.

In this paper, motivated by the objective of enabling, on a RHex-type platform, the terrain adaptive behaviors described before, we develop a proprioceptive terrain identification methodology based on the characteristic terrain signatures generated by the recently developed leg observes[11] (described in Section 2). In addition, to increase classification accuracy and robustness against leg failures, we exploit the fact that RHex-type robots employ six independently actuated legs, and propose a classification scheme that fuses, through a voting scheme, the outputs from six classifiers corresponding to each of the legs. The developed approach does not require extra sensors such us accelerometers and gyros and, unlike other proprioceptive systems, is shown to work well at robot speeds outside of the training range. Experimental results are presented on four different terrains and two different gaits. The remainder of the paper is structured as follows: Section 2 describes the experimental platform and the leg observers. Section 3 details the terrain identification methodology. Section 4 includes the experimental results. Finally, Section 5 presents concluding remarks and directions for future work.

2. EXPERIMENTAL SETUP AND LEG OBSERVERS

This section describes the robotic hexapod employed in this research and summarizes the operation of the leg observers, which are the main "sensor" employed to generate the feature vectors for the terrain identification algorithm.

2.1 Experimental Platform

The XRL (X-RHex light) robotic platform[12] shown in Fig. 1 is a very versatile, slightly lighter version of the X-RHex robot, capable of performing diverse gaits, including walking, jogging, running and pronking. The robot has 6 compliant C-shaped legs independently actuated by 50 Watt Brushless Maxon motors with a gear ratio of 18:1. The basic research platform is equipped with magnetic encoders in each leg, and sensors to monitor the currents through each of the motors. For this paper we will consider an alternating tripod gait for the XRL locomotion. Referring to Fig. 2, the alternaiting tripods correspond to a left tripod formed by legs 1,3, and 5 and a right tripod formed by legs 2,4, and 6.

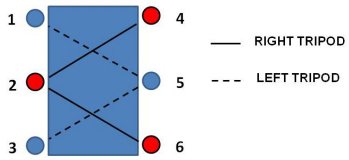

Figure 2: Left and right tripods for XRL.

Each of the tripods follows at the low level a desired trajectory generated by a Beuhler clock,[10] which characterizes the gait by four parameters: the frequency $f[Hz]$, nominal duty factor $\overline{d_f}$, nominal leg offset $\overline{\phi_o}$ [rad] and the nominal leg sweep angle $\overline{\phi_s}$ [rad]. These parameters are grouped into the control vector $u = [f, \overline{d_f}, \overline{\phi_o}, \overline{\phi_s}]^T$, where the frequency and duty factor are expressed in terms of the cycle t_c and stance t_s times by ($f = \frac{1}{t_c}$ and $\overline{d_f} = \frac{t_s}{t_c}$).

2.2 Leg Observers

Recent work on disturbance identification for RHex platforms (e.g., identification of expected ground contact, leg fault, or unexpected ground contact) has resulted in the development of leg observers that generate estimates of the leg angles, velocities, and motor currents through the usage of a model of the motor and controller employed to track the desired leg trajectories.[11] As shown in the block diagram of Fig. 3, the leg flight model has the form of a single, decoupled, servo motor driven by an estimated error, $\hat{e}$. This error has three different components $\hat{e_p}, \hat{e_d}$, and $\hat{e_g}$, which arise from a PD control law and a known reference error that captures the effects of gravity on the leg. The error terms are given by:

$$\hat{e_p} = K_p(\theta_d - \hat{\theta}), \tag{1}$$

$$\hat{e_d} = K_d(\omega_d - \hat{\omega}), \tag{2}$$

$$\hat{e_g} = K_g \sin(\hat{\theta} + \theta_g), \tag{3}$$

where K_p and K_d are proportional and derivative constants, K_g is the magnitude of the gravitational effect and θ_g is the angular offset. K_τ is the motor torque constant, R is the electrical resistance of the motor, and K_b is a damping coefficient. Finally, there is a time delay T_{del} that synchronizes the observer with the physical plant. For details pertaining the the calibration of the remaining constants $(K_p, K_d, T_{del}, K_m, A_m)$ please refer to.[11] The outputs of this observer, $\hat{\theta}$, $\hat{\omega}$, and $\hat{I}$, are compared with the actual achieved angle θ, angular velocity ω, and motor current I to form the observer residual vector:

$$\begin{bmatrix} r_\theta \\ r_\omega \\ r_I \end{bmatrix} = \begin{bmatrix} \hat{\theta} - \theta \\ \hat{\omega} - \omega \\ \hat{I} - I \end{bmatrix}. \tag{4}$$

The normalizing effect of the leg observers is illustrated in Fig. 4, which compares motor current signals of one leg vs. the current residuals (r_I) generated by the leg observer. Notice that the observer significantly reduces the current peak presented at the beginning of the flight phase. This current spike is caused due to the oscillatory motion of the leg when it leaves the ground. Besides reducing this undesirable effect, the observer residual is also closer to zero for the later portion of the flight phase (also shown in Figs. 6 and 8). Therefore, the output of the observer is a closer approximation to the motor current (torque) resulting of the leg-ground interaction on a particular terrain. Thus, we select r_I as the proprioceptive "software sensor" for terrain classification.

3. TERRAIN IDENTIFICATION AND DATA COLLECTION

In this section the generic framework employed for terrain identification is briefly summarized. In addition, the data collection process on the XRL robot is described together with an analysis of the selected feature vectors employed in the terrain identification task.

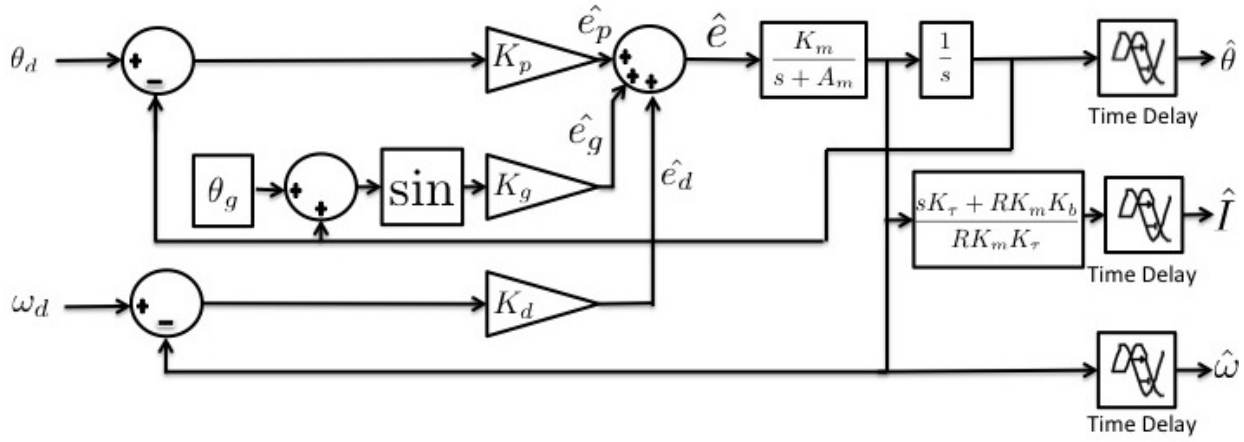

Figure 3: Block diagram of leg observer. The estimated angle $\hat{\theta}$, angular velocity $\hat{\omega}$, and motor current $\hat{I}$ are generated from the same reference angle θ_d and velocity ω_d as the actual leg using a model of the motor and controller.

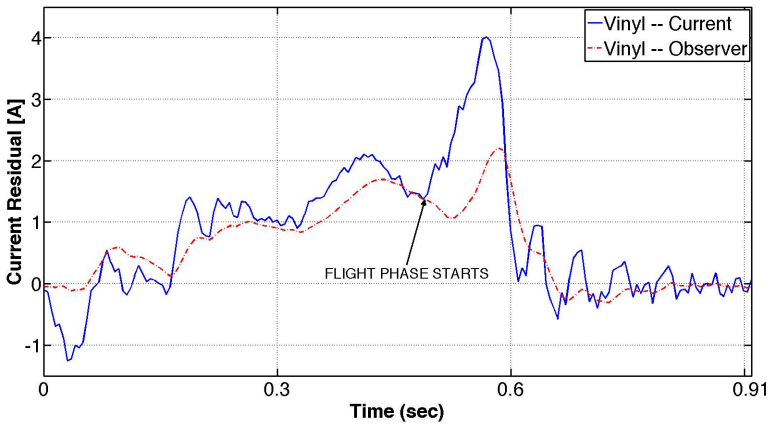

Figure 4: Comparison of current and observer residual r_I for a vinyl surface. Notice how the observer residual "cancels out" the flight dynamics ($r_I \approx 0$ for the later section of the flight phase) by utilizing models of the leg and of the trajectory tracking controller.

3.1 Terrain Identification Methodology

Motivated by previous findings on wheeled robots, which show that frequency domain features derived from Inertial Measurement Units (IMUs)[2,3] and structured light sensors[13] constitute effective terrain signatures and yield high terrain classification accuracies, here we explore the feasibility of terrain identification using the magnitude of the frequency response of the observer current residuals. In addition to providing a distinct signature of the leg-terrain interaction, leg observers are interesting for classification purposes because they are already being used in RHex-type robots to monitor the proper operation state of the robot legs. That is, the observers can be used to automatically stop the terrain classification module (or a part of it) in case of a leg failure or an early leg touchdown due to an obstacle.[11]

Fig. 5 describes at a high level the proposed terrain identication framework for multilegged platforms. The employed methodology is composed of three separate processes: a training, a testing, and an optional fusion process. In this paper, the classification block is handled by a Probabilistic Neural Network (PNN)[2] trained with previously recorded observer current residual samples captured on different terrains. Following Fig. 5, given the robot gait G_i, a separate classifier is trained per leg by using a training sample set, consisting of X

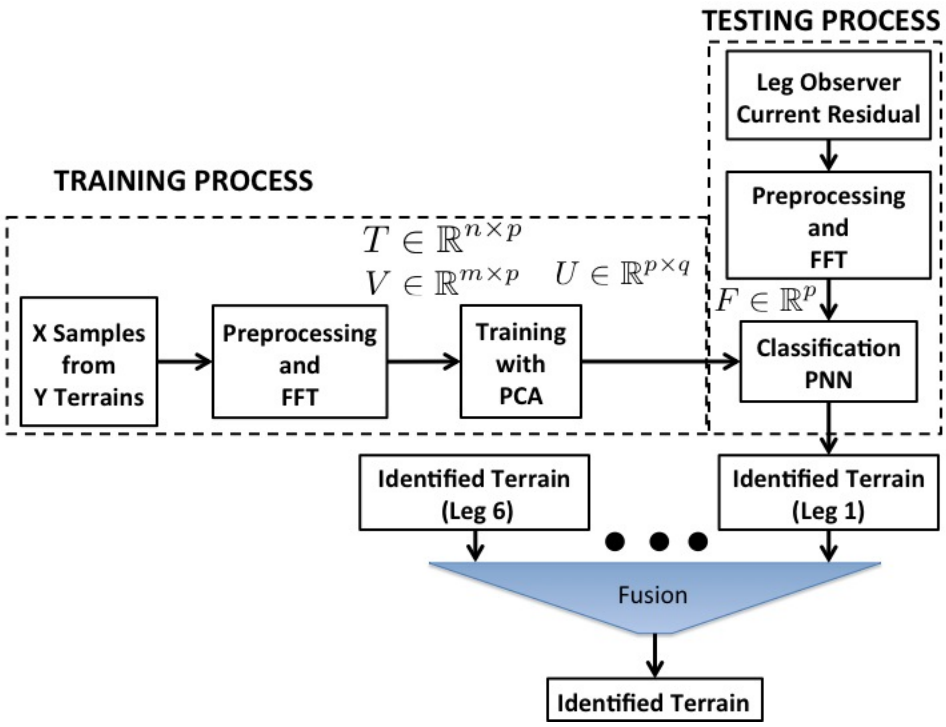

Figure 5: Terrain Identification framework for multilegged robots. The process is divided into three sections: a training process, where previously recorded terrain data is used to train parameters for classification, a testing process, where data streaming from the robot is processed for classifcation at the leg level, and an optional fusion module that combines the classification results from the different legs.

samples on Y terrains collected at different gait frequencies f_j. The training data undergoes a preprocessing stage, necessary to handle time domain signals of different lengths and reduce speed dependency of the classifier. In this stage the observer residuals collected using the higher gait frequencies are stretched and resampled via interpolation. By doing this, all signals of a particular gait will have the same length as those gathered at the lowest frequency. In addition, an important effect of this step is to reduce the speed dependency of the classifier. This is achieved because, given a particular terrain, observer residuals from high frequency gaits will be aliased with those corresponding to the low frequencies. After the preprocessing stage, the training samples are converted into a training feature matrix $T \in \mathbb{R}^{n \times p}$ and a validation feature matrix $V \in \mathbb{R}^{m \times p}$. The dimension m and n in the training and validation feature matricies F and V are equal to the total number of samples used, and p is the dimension of the feature vector (for details about the trainning process and utilization of the matrices T and V please refer to[3, 13]). In the case illustrated in Fig. 5, the feature vectors consist of the magnitude of the Discrete Fourier Transform of the leg observer current residuals.

The training process involves learning the parameters of the PNN network and a transformation matrix $U \in \mathbb{R}^{p \times q}$, trough Principal Component Analysis (PCA), which is used to reduce the dimension of the feature vector from p to q and speeds up the classification computation time. The testing process consists of gathering, over the course of a stride, an unknown terrain sample from each leg observer current residual, transforming (via the FFT) the time domain signal to a feature vector $F \in \mathbb{R}^p$, and then inputting the feature vector into the trained PNN classifier, which results in an identification for the unknown terrain sample for the particular leg l_k. Finally, an optional fusion module described later in Section 4 can be used to combine the identification results of two or more legs.

3.2 Data Collection

During the data collection process two gaits G_1 and G_2 were employed. These two gaits correspond to slow and high speed walking gaits and result in significantly different leg-terrain interaction dynamics as shown later in Figs. 8 and 9. Following the convention detailed in Section 2, the gaits are parametrized by $G_1 = [f_1, 0.53, -0.5, 1.12]$, with $f_1 \in [0.7, 1.1]Hz$ and $G_2 = [f_2, 0.46, -0.25, 0.62]$, with $f_2 \in [1.3, 1.7]Hz$. These gaits were selected to produce qualitatively stable and smooth locomotion behaviors. Table 1, presents the average forward speed of the robot corresponding to the different gait frequencies for the vinyl surface.

Table 1: Average sagital speed for different gait frequencies on a vinyl surface

Gait	G_1	G_1	G_2	G_2
Frequency[Hz]	0.7	1.1	1.3	1.7
Speed[m/s]	0.20	0.30	0.35	0.51

Observer data was gathered by commanding XRL with gait G_1 at frequencies $f_1 = \{0.7, 1.1\}Hz$ and G_2 at $f_2 = \{1.3, 1.7\}Hz$. The terrains considered in this work consist of common vinyl floor tiling, newly poured road asphalt, thick grass, and smooth small (less than $5cm$ in diameter) garden pebbles. The terrains were relatively flat and homogeneous. Several runs were conducted until 125 strides were collected for each gait and each terrain.

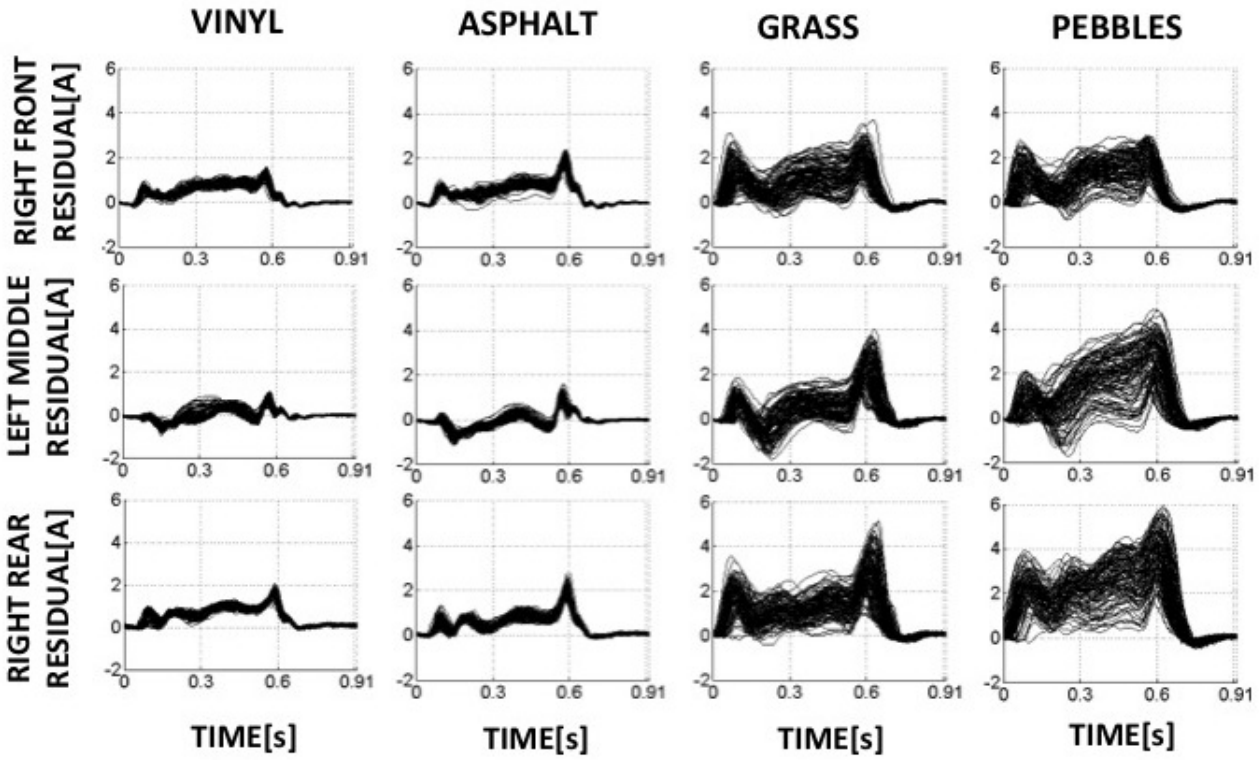

Figure 6: Observer signals for 125 strides on the four terrains (Vinyl, Asphalt, Grass, and Pebbles) tested with the XRL using gait G_1 at $f_1 = 1.1Hz$. The three rows of plots represent: right front leg, left middle leg, and right rear leg, which make up the right tripod leg set.

Figures 6 and 7 depict the terrain signatures (observer residuals) in the time and frequency domain for the right tripod leg set (data from gait G_1 at $f_1 = 1.1Hz$). From the time domain, it is possible to observe that vinyl and asphalt produce observer residuals of similar characteristics. In addition, the high variance between the 125 time domain samples for the grass and pebbles terrains are an indication of the challenges to differentiate between these two terrains. From Fig. 7, it is clear that the frequency signature of the observer residual is heavily

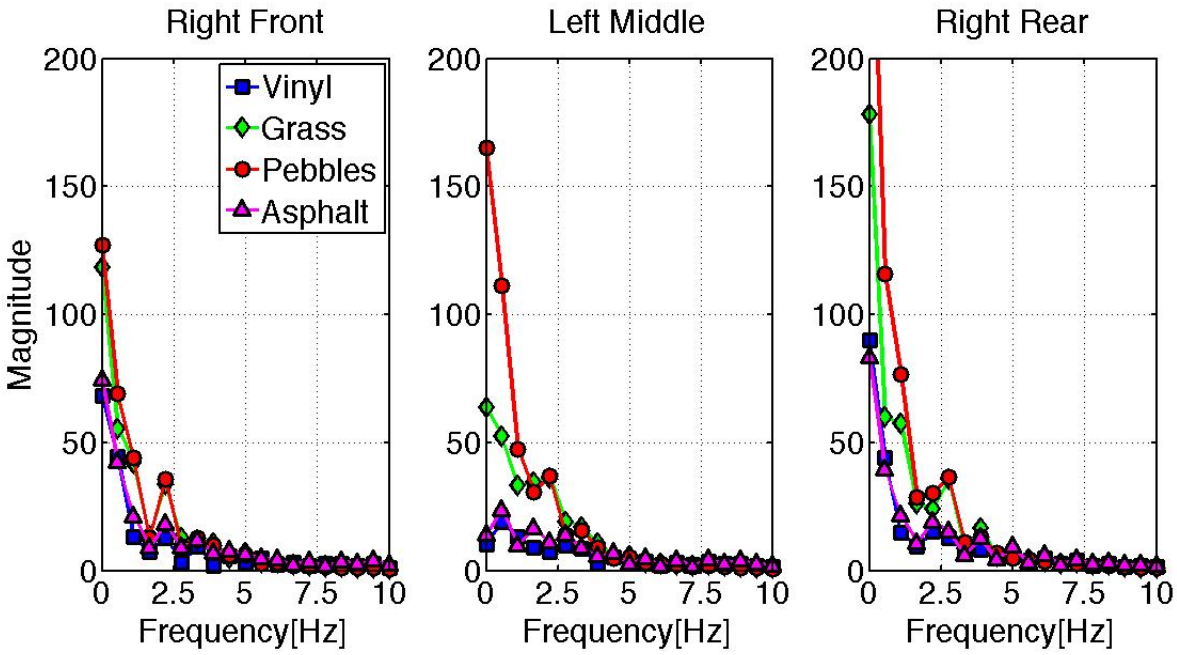

Figure 7: Average (over 125 strides) frequency domain feature vectors for each of the four terrains on the right tripod leg set. As can be seen in the plots, greater variance between terrain feature vectors is observed on the middle and back legs. The greater the variance between the different terrains, the better the probability for high terrain identification results (refer to Fig. 10).

dependent on the leg. In particular, greater variance between terrain feature vectors is observed on the middle and back legs. This observation suggests that terrain classification will be more accurate on these legs than on the front legs (refer to Fig. 10). The dissimilarity between feature vectors for the different legs also indicates that terrain classification on a particular leg should be performed with only data generated from that leg. Figure 7 also shows that, as expected, vinyl and asphalt yield flatter frequency responses. This is particularly true for the middle legs. It is also important to note that even though the average frequency responses of grass and pebbles exhibit significant differences, these terrains are easily miss classified due to the high variance of the signatures.

Figure 8 plots all 125 time domain observer signals on the left middle leg for different gait frequencies. Similarly, Fig. 9 presents the average frequency response of the observer residuals corresponding to the middle left leg. From the time and frequency domain analysis, it is clear that the terrain signatures vary significantly in shape between the two tested leg gaits Slow Walking ($G_1, f_1 = 0.7Hz$) and Fast Walking ($G_2, f_2 = 1.3Hz$). This signal variance is a strong indication that the classifier will have difficulty generalizing properly from one gait to another. A trained set of parameters for the PNN classifier must therefore be developed for each XRL gait. Although undesirable, this is not a major problem because the gaits are designed for locomotion within a certain velocity range, and are switched only when the desired operating velocity falls outside the bounds of the current gait. Therefore, when the XRL gait is changed, the trained parameters of the classifier can be updated to match the new gait.

4. EXPERIMENTAL RESULTS

As outlined in Section 3, the terrain classification process takes a set number of samples on each terrain to train the classifier parameters. Terrain samples, not used in that process, are employed to determine the accuracy of the trained classifier. The PNN classifier was trained with 75 of the recorded 125 samples from each of the four terrains. The 75 samples were further divided into 50 samples for the training feature matrix T and 25 samples for the validation matrix V. In this particular problem, PCA did not reduce the dimension of the feature vectors. With the 50 samples from each terrain not used in the training process, the terrain identification accuracy of the

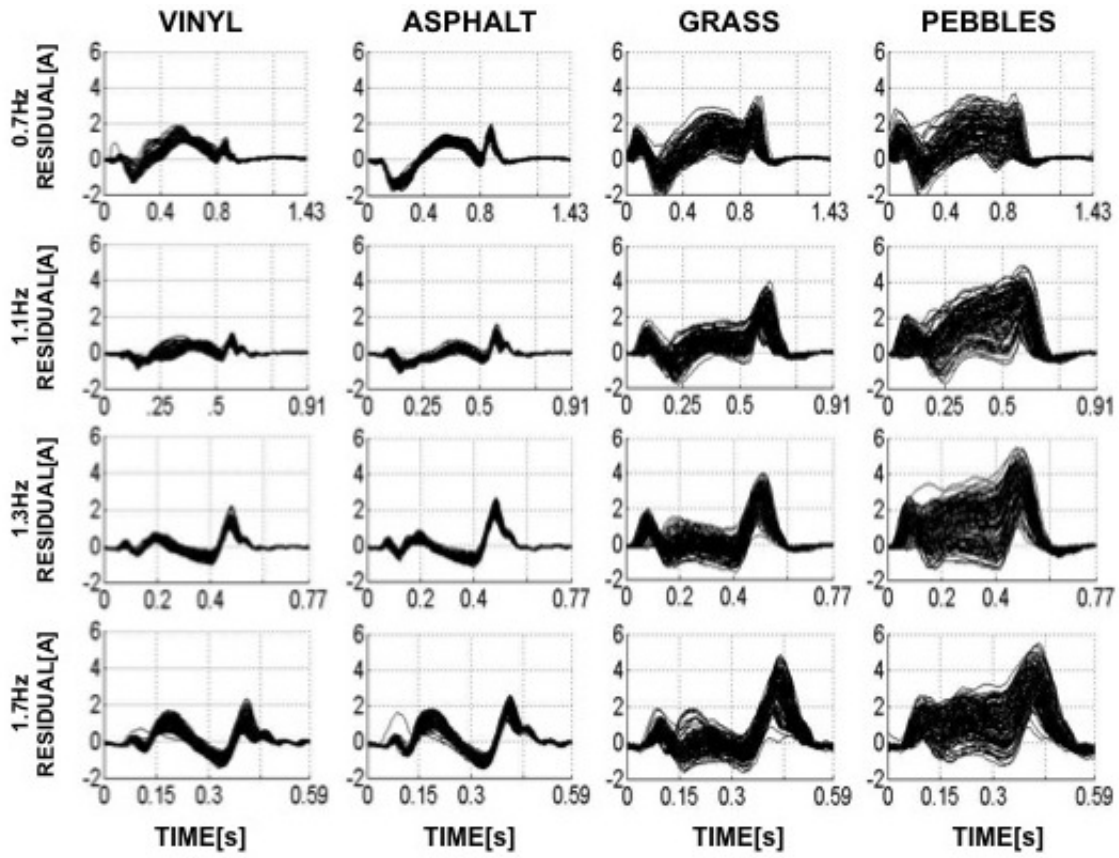

Figure 8: Observer signals on the middle left leg for different gait frequencies. The first two rows correspond to gait G_1 and the last two to gait G_2.

classifier is determined. When the samples are classified, their actual terrain type (which is known) is used to verify the terrain type identified with the classifier. Terrain identification accuracies are determined by dividing the number of correctly identified terrain samples with the number of samples tested.

For the reasons exposed in Section 3, six different classifiers were trained (one per leg). The results, displayed in Fig. 10 correspond to gait G_1 at frequency $f_1 = 1.1Hz$, and show classification accuracies in the mid-range of [78%, 90%]. As predicted from the frequency signtures of Fig. 7, the terrain identification accuracy increases from the front to the rear legs.

To improve the PNN classifier mid-range accuracy, to a high accuracy value (above 90%), the identification results from all six legs were combined using a simple yet effective voting strategy. Intuitively, using all six XRL legs to indentify terrains instead of relying on one leg, should result in higher terrain classification accuracy. Once both right and left leg tripods have completed two full consecutive steps, the twelve resulting classified terrains (one from each leg per stride) are tallied, and the terrain with the majority of votes becomes the outputted identified terrain. The identified terrain is defaulted to the rougher terrain for the occasions when there is a tie in the tally. For example, a tie between terrains asphalt and grass will default the output terrain to grass. As already mentioned, in this preliminary study, two full strides of the robot were employed for classification. However, techniques such as the control update rules for wheeled vehicles, could be adapted to find the optimal number of strides that should be used in the fusion block.[13,14]

The confusion matrix in Table 2, depicts the accuracies attained through the voting strategy when the classifier is tested at the same gait frequency that was used during training. Table 2, displays both the success rate and miss-classifications on each of the four tested terrains. In the case of (G_1,$f_1 = 1.1Hz$), the overall

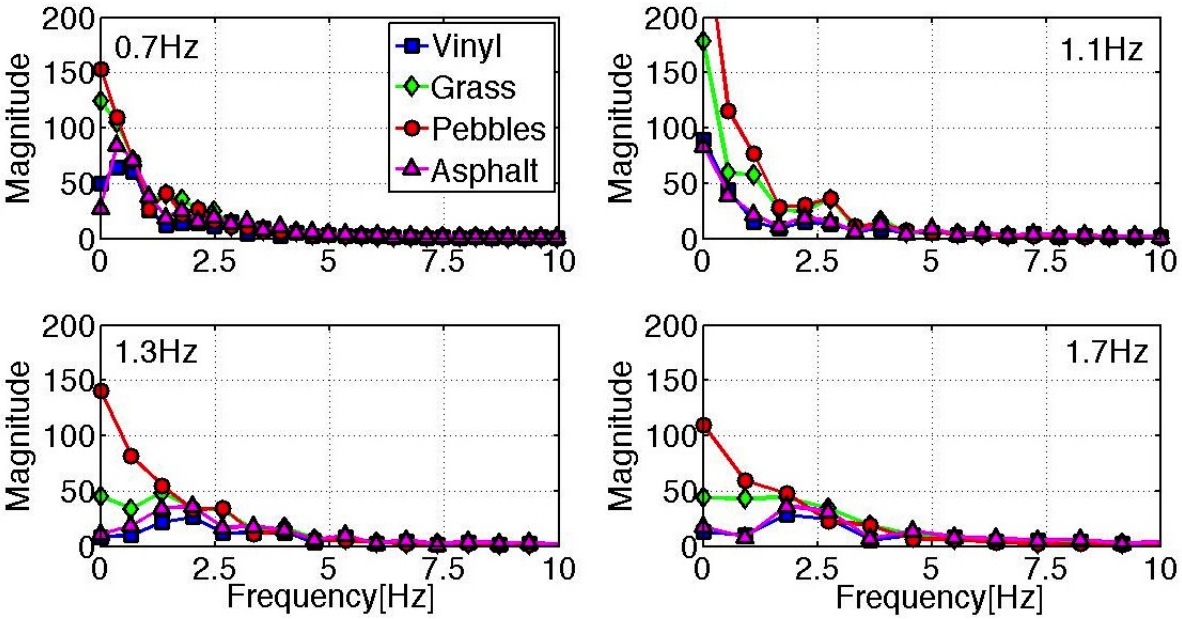

Figure 9: Average frequency response of the observer residuals as a function of gait frequency. The first row corresponds to gait G_1 and the second row corresponds to gait G_2 (all data is obtained from the middle left leg).

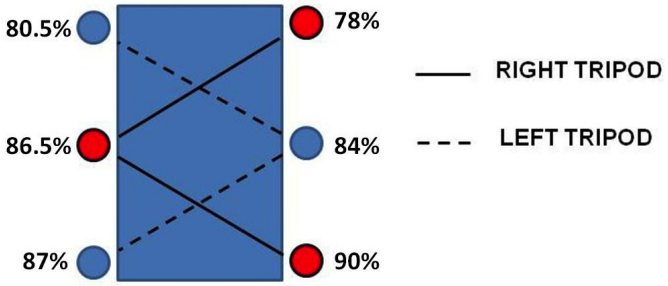

Figure 10: The overall terrain identification accuracies achieved on each of the six XRL legs on four terrains (Vinyl, Asphalt, Grass, and Pebbles). These results where obtained employing gait G_1 at $f_1 = 1.1Hz$.

terrain identification accuracy (OA) (computed from the confusion matrix diagonal) is 96%, a 6% improvement when compared to the highest, 90%, accuracy from using just the back right leg. Note, in Table 2 that the terrains grass and pebbles are still miss-classifying each other. However, the vinyl and asphalt terrains depict perfect 100% accuracy. Hence forth, throughout this paper terrain classification accuracies are computed using the proposed voting strategy over two consecutive XRL strides.

Table 2: Terrain identification results for gait G_1 employing the voting strategy

		$f_1 = 0.7Hz$ (OA = 83%)				$f_1 = 1.1Hz$ (OA = 96%)			
		V	A	G	P	V	A	G	P
Detected Terrain	V	100%		4%	12%	100%			
	A		100%				100%		
	G			80%	36%			100%	16%
	P			16%	52%				84%

Table 3: Terrain identification results for gait G_2 employing the voting strategy

		$f_2 = 1.3Hz$ (OA = 91%)				$f_2 = 1.7Hz$ (OA = 93%)			
		V	A	G	P	V	A	G	P
Detected Terrain	V	100%				100%			
	A		100%				100%	12%	
	G			92%	28%			84%	12%
	P			8%	72%			4%	88%

In order to test the dependency of the classification results on gait frequency (speed), four classifiers C_i with $i = \{1, 2, 3, 4\}$ were trained at the lowest and highest frequencies for each gait. Then, the classifiers were tested with data gathered employing the frequency that was not used in training. Tables 4 and 5 summarize the combinations used for training and testing. This experiment yielded poor overall identification accuracies (63% for C_1, 62% for C_2, 51% for C_3 and 61% for C_2), which shows that the classifiers generalize poorly between the frequency boundaries of the gaits.

Table 4: Combinations used during training to test dependency of classification results on gait frequency.

Classifier	C_1	C_2	C_3	C_4
Gait	G_1	G_1	G_2	G_2
Frequency[Hz]	0.7	1.1	1.3	1.7

Table 5: Combinations used during testing to study dependency of classification results on gait frequency.

Classifier	C_1	C_2	C_3	C_4
Gait	G_1	G_1	G_2	G_2
Frequency[Hz]	1.1	0.7	1.7	1.3

To alleviate this exposed frequency dependence without incurring in prohibitively extensive experimentation at many gait frequencies, an additional experiment was conducted for gait G_2 (notice that G_2 yielded the worst overall accuracies $(51\%, 61\%)$ in the previous experiment). In this case, a classifier was trained using gait G_2 combining data from both frequency boundaries ($f_2 = \{1.3, 1.7\}Hz$). Then, the classifier was tested at all 3 speeds, including an intermediate frequency $f_2 = 1.5Hz$. Table 6 summarizes the confusion matrix from this experiment. Notice that high overall accuracy and low miss-classifications are obtained at the intermediate gait frequency.

Table 6: Terrain identification results for gait G_2 when testing at an intermediate gait frequency not included in the training set. The classifier was trained with data gathered at gait frequencies of 1.3 and 1.7Hz.

		$f_2 = 1.3Hz$ (OA=91%)				$f_2 = 1.5Hz$ (OA=93.8%)				$f_2 = 1.7Hz$ (OA=92%)			
		V	A	G	P	V	A	G	P	V	A	G	P
Detected Terrain	V	100%				100%		8.3%	8.3%	100%			
	A		100%				100%	8.3%			100%	16%	
	G			88%	24%			83.3%				80%	12%
	P			12%	76%				91.7%			4%	88%

5. CONCLUSIONS AND FUTURE WORK

Motivated by the future goal of enabling the terrain dependent behaviors described in Section 1, a new proprioceptive terrain identification methodology was proposed. The approach is based on the frequency response of the leg observers current residuals and is particularly suited for multilegged systems with minimal sensing because

it does not require additional sensors such as accelerometers, gyroscopes, and lasers. Experimental verification was performed on the XRL platform utilizing two gaits with significantly different leg dynamics, and on four different terrains. It was found that each leg of the hexapod generates very distinct observer residuals in the time and frequency domains, which motivated the inclusion of six independent classifiers (one per leg). Of particular interest are the findings that the middle and rear legs lead to better separation of the terrain signatures and therefore yield better classification results when compared to the front legs. With the objective of increasing overall classification accuracy and robustness against leg failure, a simple voting strategy that combines the outputs of the six independent classifiers was implemented and found to produce significant improvement.

In addition to leg dependency, a major challenge on terrain classification for legged robots is the speed dependency of the terrain signatures. To cope with this, the proposed methodology trains the classifier utilizing data gathered at the minimum and maximum gait frequencies. This process, together with the voting scheme, results in good generalization for intermediate gait frequencies. In fact, it is almost as good as an over specialized classifier (i.e., a classifier trained and tested at the same gait frequency).

Future work, will include the fusion of the current frequency domain feature vectors with additional features derived from the time domain signals generated by the leg observers (e.g., stride-to-stride variance). In addition, the classifier will be evaluated with faster running gaits, which are expected to produce much richer terrain signatures and therefore improve the classification results. We will also proceed with the online implementation of the proposed approach and its integration with some of the terrain adaptive behaviors described in Section 1. Finally, we will evaluate the feasibility of integrating the leg observers with additional technologies such us contact-based sensing of the terrain with the Pressure Sensitive Robotic Skin (PreSRS), which is used to measure the pressure distribution across a surface and has been shown to produce excellent terrain classification results on a single leg hopper.

6. ACKNOWLEDGMENT

This work was supported by the collaborative participation in the Robotics Consortium sponsored by the U.S. Army Research Laboratory under the Collaborative Technology Alliance Program, Cooperative Agreement DAAD 19-01-2-0012, and funded by National Science Foundation under Award CMMI-0927040. The U.S. Government is authorized to reproduce and distribute reprints for Government purposes not withstanding any copyright notation thereon.

REFERENCES

1. A. Howard and H. Seraji, "Vision-based terrain characterization and traversability assessment," *Journal of Robotic Systems* **18**, pp. 557–587, 2001.
2. E. DuPont, C. Moore, E. Collins, and E. Coyle, "Frequency response method for terrain classification in autonomous ground vehicles," *Autonomous Robots* **24**, pp. 337–347, 2008.
3. E. DuPont, E. Collins, E. Coyle, and R. Roberts, *Terrain classification using vibration sensors: theory and methods*, Nova Science Publishers, Inc., 2010.
4. E. Krotkov, "Active perception for legged locomotion: Every step is an experiment," in *Proceedings of the IEEE International Symposium on Intelligent Control*, pp. 227–232, 1990.
5. M. Hoepflinger, D. Remy, M. Hutter, L. Spinello, and R. Siegwart, "Haptic terrain classification for legged robots," in *Proceedings of the IEEE International Conference on Robotics and Automation*, 2010.
6. P. Filitchkin and K. Byl, "Feature-based terrain classification for littledog," in *Proceedings of the IEEE/RSJ International Conference on Intelligent Robots and Systems*, 2012.
7. P. Giguere, G. Dudek, C. Prahacs, and S. Saunderson, "Environment identification for a running robot using inertila and actuator cues," in *Proceedings of the Robotics Science and Systems (RSS)*, 2006.
8. S. Manjanna, G. Dudek, and P. Giguere, "Using gait change fo terrain sensing by robots," in *Tenth Conference on Computer and Robot Vision (CRV)*, (Regina, Canada), 2013.
9. F. Garcia, R. Julian, D. Haldane, P. Abbeel, and R. Fearing, "Performance analysis and terrain classification for a legged robot over rough terrain," in *Proceedings of the IEEE/RSJ International Conference on Intelligent Robots and Systems*, 2012.

10. U. Saranli, M. Buehler, and D. E. Koditschek, "Rhex: A simple and highly mobile hexapod robot," *International Journal of Robotics Research* **20**(7), pp. 616–631, 2001.
11. A. M. Johnson, G. C. Haynes, and D. E. Koditschek, "Disturbance detection, identification, and recovery by gait transition in legged robots," in *Proceedings of the IEEE/RSJ Intl. Conference on Intelligent Robots and Systems*, (Taipei, Taiwan), 2010.
12. G. C. Haynes, J. Pusey, R. Knopf, A. M. Johnson, and D. E. Koditschek, "Laboratory on legs: an architecture for adjustable morphology with legged robots," in *Proceedings of the SPIE Defense, Security, and Sensing Conference, Unmanned Systems Technology XIV*, **8387**(1), 2012.
13. L. Lu, C. Ordonez, E. Collins, E. Collins, E. Coyle, and D. Palejiya, "Terrain surface classification with control mode update rule using a 2d laser stripe-based structured light sensor," *Robotics and Autonomous Systems* **59**, pp. 954–965, 2011.
14. E. Coyle and E. Collins, "Updating control modes based on terrain classification," in *Proceedings of the IEEE Conference on Robotics and Automation*, pp. 4417–4423, (Anchorage, AK), May 3-5 2010.